Unraveling the protective mechanisms of Chuanfangyihao against acute lung injury: Insights from experimental validation

HONGFANG FU[1,2*], XIAO LIANG[2*], WANYING TAN[1,2] and XIAOYU HU[1]

[1]Infectious Disease Department, Hospital of Chengdu University of Traditional Chinese Medicine; [2]School of Clinical Medicine, Chengdu University of Traditional Chinese Medicine, Chengdu, Sichuan 610072, P.R. China

Received June 25, 2023; Accepted August 21, 2023

DOI: 10.3892/etm.2023.12234

Abstract. Chuanfangyihao (CFYH) is an effective treatment for acute lung injury (ALI) in clinical practice; however, its underlying mechanism of action remains unclear. Therefore, the aim of the present study was to elucidate the pharmacological mechanism of action of CFYH in ALI through experimental validation. First, a rat model of ALI was established using lipopolysaccharide (LPS). Next, the pathological changes in the lungs of the rats and the pathological damage were scored. The wet/dry weight ratios were measured, and ROS content was detected using flow cytometry. ELISA was used to examine IL-6, TNF-α, IL-1β, IL-18, and LDH levels. Immunohistochemistry was used to detect Beclin-1 and NLRP3 expression. Western blotting was performed to analyze the expression of HMGB1, RAGE, TLR4, NF-κB p65, AMPK, p-AMPK, mTOR, p-mTOR, Beclin-1, LC3-II/I, p62, Bcl-2, Bax, Caspase-3, Caspase-1, and GSDMD-NT. The mRNA levels of HMGB1, RAGE, AMPK, mTOR, and HIF-1α were determined using reverse transcription quantitative PCR. CFYH alleviated pulmonary edema and decreased the expression of IL-6, TNF-α, TLR4, NF-κB p65, HMGB1/RAGE, ROS, and HIF-1α. In addition, pretreatment with CFYH reversed ALI-induced programmed cell death. In conclusion, CFYH alleviates LPS-induced ALI, and these findings provide a preliminary clarification of the predominant mechanism of action of CFYH in ALI.

Correspondence to: Professor Xiaoyu Hu, Infectious Disease Department, Hospital of Chengdu University of Traditional Chinese Medicine, 39 Twelve Bridges Road Qiao Road, Jinniu, Chengdu, Sichuan 610072, P.R. China
E-mail: hu.xiaoyuhu@aliyun.com

*Contributed equally

Abbreviations: ALI, acute lung injury; ARDS, acute respiratory distress syndrome; CFYH, Chuanfangyihao; Dex, Dexamethasone; W/D, ratio of wet weight to dry weight; DCFH-DA, 2',7'-dichlorofluorescein diacetate

Key words: Chuanfangyihao, acute lung injury, acute respiratory distress syndrome, experimental validation, traditional Chinese medicine

Introduction

Acute lung injury (ALI) is a hyper-inflammatory syndrome characterized by progressive dyspnea and refractory hypoxemia. It is caused by various pathogenic factors, both internal and external to the lung (1). These factors contribute to the dysregulation of lung function, leading to the development of ALI. Moreover, when the condition of patients with ALI deteriorates and the oxygenation index decreases to $PaCO_2/FiO_2$ ≤200 mmHg (1 mmHg=0.133 kPa), severe acute respiratory distress syndrome (ARDS) develops (2). ALI and ARDS are the leading causes of acute respiratory failure, with an incidence of 789 per 100,000 people per year in the United States, according to a report in 2005 (3). Globally, the mortality rate for ALI and ARDS is 30-40% (4). While the cascade of inflammation is considered the typical pathogenesis of ALI/ARDS, there are still several controversies surrounding this mechanism (5). Based on the pathophysiological changes and clinical manifestations of ALI/ARDS, its treatment measures can be divided into mechanical ventilation support and drug therapy (6-8). Mechanical ventilation adopts a protective lung ventilation strategy, which is considered the cornerstone of the treatment of ALI/ARDS (9). Drug therapy primarily includes anti-inflammatory agents, antioxidants, vasodilators, and lung surfactants (10). Unfortunately, despite significant progress in treatment methods for ALI/ARDS, the clinical mortality rate remains high (11). Therefore, there is an urgent to identify safe and effective treatment methods. In recent years, with the deepening research on the prevention and treatment of ALI/ARDS using traditional Chinese medicines (TCMs), numerous basic studies have demonstrated the beneficial effects of TCM on ALI/ARDS (12). CFYH is a TCM formula that was developed for ALI, which consists of the following ingredients: *Poria Cocos* (*Schw.*) *Wolf.* (Fu ling), *Zingiber Officinale Roscoe* (Sheng jiang), *Atractylodes Macrocephala Koidz.* (Bai zhu), *Typhonii Rhizoma* (Fu zi), *Hedysarum Multijugum Maxim.* (Huang qi), Angelicae Sinensis Radix (Dang gui), *Radix Paeoniae Rubra* (Chi shao), *Pheretima Aspergillum* (Di long), *Chuanxiong Rhizoma* (Chuan xiong), *Carthami Flos* (Hong hua), and *Persicae Semen* (Tao ren). CFYH is designed to remove water from the lungs, and relieve coughs and asthma.

Our previous clinical studies have confirmed that CFYH is effective for the treatment of ALI/ARDS, and it has been shown to reduce the risk of progression to severe disease (13,14). In the present study, the underlying mechanisms of action of CFYH in ALI/ARDS were assessed to provide evidence-based support for its integration into clinical practice, increasing treatment options and improving patient outcomes.

Materials and methods

Reagents. LPS (cat. no. 0000081275; purity>99% by HPLC) was purchased from MilliporeSigma. Dexamethasone acetate tablets (Dex; cat. no. H51022823; 0.75 mg/tablet) were obtained from Chengdu No. 1 Pharmaceutical Co. Ltd. BCA Protein Concentration Determination Kit (cat. no. MA0082), Rapid Gel Kit (cat. no. MA0159), and ECL chemiluminescence kit (cat. no. MA0186) were purchased from Dalian Meilun Biotechnology Co., Ltd. The cDNA First Strand Synthesis Kit (cat. no. FP205) and 2x SYBR Green PCR MasterMix (cat. no. KR118) were purchased from Tiangen Biochemical Technology Co., Ltd. RNA Extraction Kit (cat. no. R1200) was purchased from Beijing Solarbio Technology Co., Ltd. ELISA kits for IL-6 (cat. no. 22A109), TNF-a (cat. no. 22A116), and IL-1β (cat. no. ITWE8PMAF6) were purchased from Excell Biochemical Technology Co., Ltd. Antibodies against NF-κB p65 (cat. no. 380172), HMGB1 (cat. no. R22773), RAGE (cat. no. 381618), HIF-1α (cat. no. 340462), AMPK α1 (cat. no. 380431), phospho-AMPK α1 (Thr183)/AMPK α2 (Thr172) Rabbit pAb (cat. no. 383462), mTOR/phospho-mTOR (Ser2481) Rabbit pAb (cat. no. 381548), LC3A/B (cat. no. 306019), Bax (cat. no. 380709) and SQSTM1/p62 Rabbit mAb (cat. no. R27312) were purchased from Chengdu Zhengneng Biotechnology Co., Ltd. Antibodies against TLR4 (cat. no. AF7017), NLRP3 (cat. no. DF7438), GSDMD-NT (cat. no. AF4012), and caspase-3 were obtained from Affinity Biologicals Co., Ltd. Reactive oxygen Species testing kit (cat. no. S0033S) was purchased from Shanghai Biyuntian Biotechnology Co., Ltd. LDH (cat. no. 20210803) was obtained from Nanjing Jiancheng Biological Co., Ltd. Antibodies against Beclin-1 (cat. no. 11306-1-AP), Bcl2 (cat. no. 26593-1-AP), Caspase-1/P20/P10 Polyclonal Antibody Bcl2 Polyclonal Antibody (cat. no. 26593-1-AP), Caspase-1/P20/P10 Polyclonal Antibody (cat. no. 22915-1-AP) were obtained from Wuhan Sanying Biotechnology Co., Ltd. Rat IL-18 (cat. no. E-EL-R0567c) was purchased from Wuhan Elite Biotechnology Co. Ltd.

Preparation of CFYH. The drug composition of CFYH is shown in Table I. The Chinese herbal medicines that constitute CFYH were provided by the Sichuan New Green Pharmaceutical Technology Development Co., Ltd. All medicinal materials were extracted twice with boiling water, combined with the filtrate, and concentrated to form a decoction (2.0 g/ml). The middle dose was calculated according to the equivalent dose in rats, which was ~6.3x that of a 70 kg adult (15). Therefore, the dose of CFYH in rats was 41.13 g/kg/day. The lowest dose of CFYH was 20.565 g/kg/day, and the highest dose was 82.26 g/kg/day. Based on the required concentration of CFYH, pure water was added and stored at room temperature until further use.

Animals and experimental design. The experimental procedure was approved by the Medical Ethics Committee of the Sichuan Academy of TCM [grant no. SYLL (2022)-039] (16). We strictly followed the replacement, reduction, and refinement principle, and adhered to the National Institutes of Health Guidelines for the Care and Use of Laboratory Animals and ARRIVE Animal Research guidelines (17). The experiments were performed as shown in Fig. 1. A total of 36 male Sprague-Dawley rats (10-week-old, weighing 180-220 g) were provided by the Experimental Animal Center of Sichuan University [license no. SCXK (Sichuan) 2018-026, certificate no. 00116050]. They were housed in specific-pathogen-free environments at the Sichuan Academy of TCM (12 h dark/light cycle; humidity, 55±5%; temperature, 25±1˚C), and provided with *ad libitum* access to a standard diet and water.

The rats were adaptively fed for 1 week and then divided into groups as follows (n=6/group): i) sham group, ii) LPS group (10 mg/kg), iii) Dex (DEX) group (0.27 mg/kg/day) (18), iv) CFYH low dose group (20.565 g/kg/day), v) CFYH medium dose group (41.13 g/kg/day), and a vi) CFYH high dose group (82.26 g/kg/day). The sham and LPS groups received oral gavage of saline (2 ml), whereas the other groups received the corresponding drugs twice daily for 5 days. A total of 12 h after the final administration, rats in the sham group were intratracheally administered normal saline (10 mg/kg), whereas those in the other groups were intratracheally administered LPS (10 mg/kg). The dosage and usage of LPS were determined based on previous literature (19,20). The preparation method was as follows: 10 mg LPS was dissolved in 10 ml normal saline and stored away from light. After a 24-h period following the establishment of the LPS model, all rats were sacrificed by injecting 3% pentobarbital sodium.

Lung wet/dry (W/D) weight ratio. After sacrificing the rats, a portion of the right lung tissue was removed and weighed to obtain the wet weight (W), and then it was dried in an 80˚C incubator for 48 h to obtain the dry weight (D).

Histological analysis. Another region of the lung tissue was soaked in 4% formaldehyde for 24 h at room temperature, embedded in paraffin, cut into 3 μm sections, and stained with hematoxylin-eosin (H&E) at room temperature for 5 min. Finally, the samples were observed at 20x magnification using a light microscope and scored. The scoring criteria were as follows: i) alveolar congestion; ii) hemorrhage; iii) infiltration or aggregation of neutrophils in airspace or vessel wall; and iv) thickness of alveolar wall/hyaline membrane formation (21). Each item was scored on a five-point scale as follows: 0, minimal damage; 1, mild damage; 2, moderate damage; 3, severe damage; and 4, maximal damage.

ROS content of lung tissue. The lung tissues were flushed with PBS, and 1 ml collagenase was added to dissociate the tissues, which were then incubated at 37˚C for 10 min. Digestion was terminated with 3% FBS and filtered with a 40-μm cell screen. Then, 10 ml PBS was added, and the mixture was centrifuged at 186 x g for 5 min at room temperature to remove the supernatant. 2',7'-dichlorofluorescein diacetate (DCFH-DA) was diluted with a serum-free medium at a ratio of 1:1,000, resulting in a final concentration of 10 μmol/l. After adding 500 μl diluted

Table I. Ingredients list of Chuanfangyihao.

Medicine	Latin name	Weight, g	Place of production in China	Batch no.
Fu ling	*Poria Cocos (Schw.) Wolf.*	9	Yunnan	21060033
Sheng jiang	*Zingiber Officinale Roscoe*	9	Sichuan	20060086
Bai zhu	*Atractylodes Macrocephala Koidz.*	6	Hebei	21030002
Fu zi	*Typhonii Rhizoma*	9	Sichuan	20120037
Huang qi	*Hedysarum Multijugum Maxim.*	40	Gansu	21030101
Dang gui	*Angelicae Sinensis Radix*	10	Gansu	21020050
Chi shao	*Radix Paeoniae Rubra*	20	Sichuan	20100082
Di long	*Pheretima aspergillum*	10	Guangxi	21030065
Chuan xiong	*Chuanxiong Rhizoma*	20	Sichuan	21050011
Hong hua	*Carthami Flos*	15	Xinjiang	21020096
Tao ren	*Persicae Semen*	15	Gansu	20040082

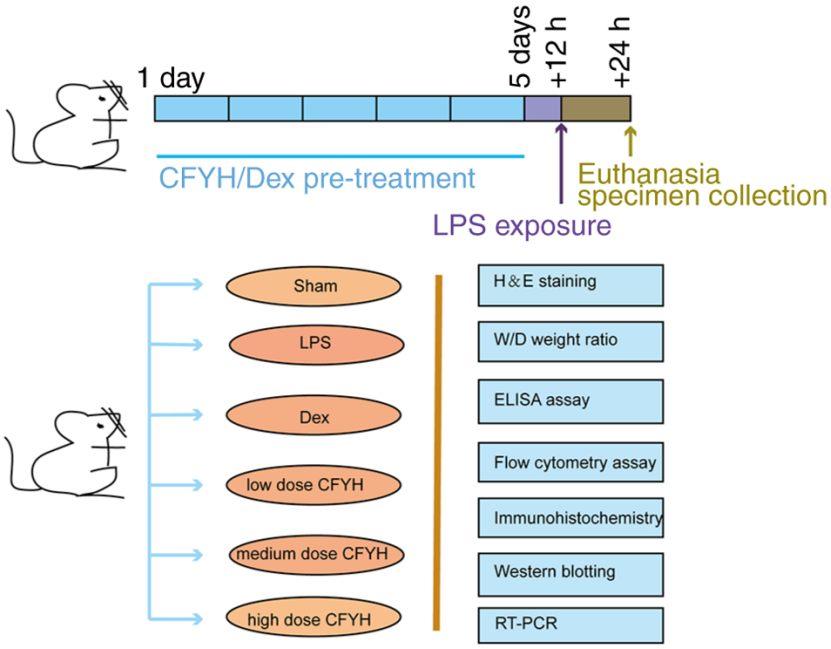

Figure 1. Schematic of the experimental protocols of the present study. CFYH, Chuanfangyihao; H&E, hematoxylin and eosin; W/D: ratio of wet weight to dry weight of lung tissue; LPS, lipopolysaccharide; RT, reverse transcription.

DCFH-DA, the samples were incubated in a cell culture box at 37˚C for 20 min. The cells were rinsed three times with serum-free cell culture medium. Finally, the cells were resuspended in PBS, and FITC fluorescence was detected using a CytoFLEX flow cytometer (Beckman Coulter, Inc.) with CytExpert software (version, 2.3.0.84; Beckman Coulter, Inc.).

ELISA. Lung tissues (100 mg) were rinsed with PBS and dried on filter paper. The lung tissue was homogenized, and the homogenate was centrifuged at 5,000 x g for 10 min at 4˚C to obtain the supernatant for analysis. TNF-α, IL-6, IL-18, IL-1β, and LDH levels were determined in the lung tissue homogenates using specific ELISA kits.

Immunohistochemistry assay. The paraffin-embedded lung sections were dewaxed with xylene and rehydrated using an ethanol gradient. The slices were completely immersed in citrate buffer and heated for 20 min at 100˚C. After cooling naturally, the samples were washed with PBS three times. The sections were incubated in 3% H_2O_2 for 20 min and washed with PBS. Then, the sections were incubated with the primary antibody for 2 h at 37˚C and washed with PBS three times. The secondary antibody was added, and the sections were incubated for 15 min and washed with PBS three times. DAB was added to the sections for color development, hematoxylin was used for re-dyeing at room temperature, and neutral glue was used to seal the sections and observed under a microscope.

Western blot analysis. Lung tissues were fully homogenized to extract proteins, and the protein concentration was determined using a BCA kit. Equal quantities of protein were separated by 10% SDS-PAGE and transferred onto PVDF membranes.

Table II. Sequences of the primers.

Gene	Forward primer, 5'-3'	Reverse primer, 5'-3'
HMGB1	GCGCGCGCCAGGAAAAT	GCCTTTGATTTTTGGGCGGT
RAGE	GGGTCACAGAAACCGGTGAT	ATCATGTGGGCTCTGGTTGG
AMPK	CAAACACCAAGGCGTACG	TGCTCTACACACTTCTGCCAT
mTOR	CGTCACAATGCAGCCAACAA	AACAAACTCGTGCCCATTGC
HIF-1α	TCCTGCACTGAATCAAGAGGTTGC	ACTGGGACTGTTAGGCTCAGGTG
β-actin	CGTTGATATCCGTAAAGACC	TACATAACAGTCCGCCTAGAAG

The membranes were blocked with 5% skim milk for 1 h at room temperature, then washed three times and incubated with primary antibodies overnight at 4˚C. The following day, the membranes were washed three times with PBS for 10 min each and then incubated with a secondary antibody for 2 h at room temperature. Finally, the membrane was washed three times for 10 min. Protein bands were detected using an enhanced chemiluminescence detection kit. ImageJ (version, 1.51j8; National Institutes of Health) was used for the densitometry analysis.

Reverse transcription-quantitative (RT-q)PCR. Total RNA was extracted from rat lung tissues using a total RNA extraction kit (Beijing Solarbio Technology Co., Ltd.) according to the manufacturer's instructions. The RNA was reverse transcribed into cDNA using the FastKing cDNA first-strand synthesis kit produced by Tiangen Biochemical Technology Co., Ltd. according to the manufacturer's protocol. qPCR was then used to determine the relative expression of HMGB1, RAGE, AMPK, mTOR, and HIF-1α. Primer sequences are listed in Table II. Thermocycling conditions were as follows: 95˚C for 15 min; then 40 cycles of 95˚C for 10 sec, 55˚C for 20 sec and 72˚C for 30 sec. Compared with housekeeping gene (β-actin), the relative mRNA expression was calculated using the $2^{-\Delta\Delta Cq}$ method and expressed as the change compared with the control group (22).

Statistical analysis. SPSS version 26.0 (IBM Corp.) and GraphPad Prism version 8.0 (GraphPad Software, Inc.) were used for data processing and developing the figures. Data are presented as the mean ± SD (23). When multiple groups were compared, ANOVA was used for parametric data and Kruskal-Wallis was used for multiple groups that were non-parametric. Pair-based comparison of homogeneous variances were evaluated using Tukey's test, heterogeneous variances were determined using Dunnett's T3 test. $P<0.05$ was considered to indicate a statistically significant difference.

Results

Protective effect of CFYH on ALI

Effect of CFYH on lung histopathology. The H&E staining results (Fig. 2) showed that the lung tissue structure of rats in the sham group was normal, while that of rats in the LPS group showed thickening of the alveolar wall and widening of the alveolar septum, along with a large number of red blood cells and inflammatory cells in the alveolar cavity, and the lung tissue damage score was significantly increased. In the CFYH and Dex groups, the infiltration of red blood cells and inflammatory cells into the lung tissue decreased, and the thickness of the alveolar wall decreased. The decrease in lung tissue inflammation was most marked in the low-dose CFYH group, and the lung tissue injury score was significantly lower (Fig. 3A). The W/D weight ratio can be used to reflect pulmonary edema. The W/D weight ratio in the LPS group was substantially higher than that in the sham group. As shown in Fig. 3B, the W/D weight ratio decreased after pretreatment with CFYH and Dex, especially at low and medium doses of CFYH.

CFYH downregulates the expression of IL-6 and TNF-α in lung tissues. ALI is characterized by the presence of inflammatory cytokines. ELISA results showed that LPS exposure resulted in increased expression of IL-6 and TNF-α compared to that in the sham group. However, IL-6 was significantly reduced in the low and medium-dose CFYH group, and TNF-α was notably decreased in the low and medium-dose CFYH and Dex groups (Fig. 3C and D).

Effects of CFYH on oxidative metabolism in rats with LPS-induced ALI. ROS content was analyzed by flow cytometry, and the results revealed that ROS levels increased in the LPS group, whereas they were downregulated in the CFYH and Dex groups (Fig. 3E).

Effects of CFYH on HMGB1/RAGE signaling. Western blotting was used to detect the expression of NF-κB P65, TLR4, HMGB1, and RAGE protein expression levels. As shown in Figs. 4A-E and 5, LPS stimulation enhanced the levels of NF-κB P65, TLR4, HMGB1, and RAGE. In contrast, CFYH and Dex pretreatment markedly reversed this effect. The expression of NF-κB P65 was notably reduced in the low and medium-dose CFYH groups and Dex group. TLR4 expression also decreased in the CFYH and Dex groups. Simultaneously, HMGB1 expression in the low and medium-dose CFYH groups was markedly reduced, and the results of RT-qPCR were consistent with these results. The expression levels of RAGE in the low and medium-dose CFYH groups and Dex group were markedly decreased. The RT-qPCR results revealed that RAGE mRNA levels decreased after CFYH and Dex pretreatment. Compared with the Dex group, the low-dose CFYH group was more noticeably reduced (Fig. 4D-F).

The effect of CFYH on HIF-1α was analyzed by PCR; LPS resulted in HIF-1α upregulation, but pretreatment with CFYH inhibited these effects, especially in the low and medium-dose groups (Fig. 3F).

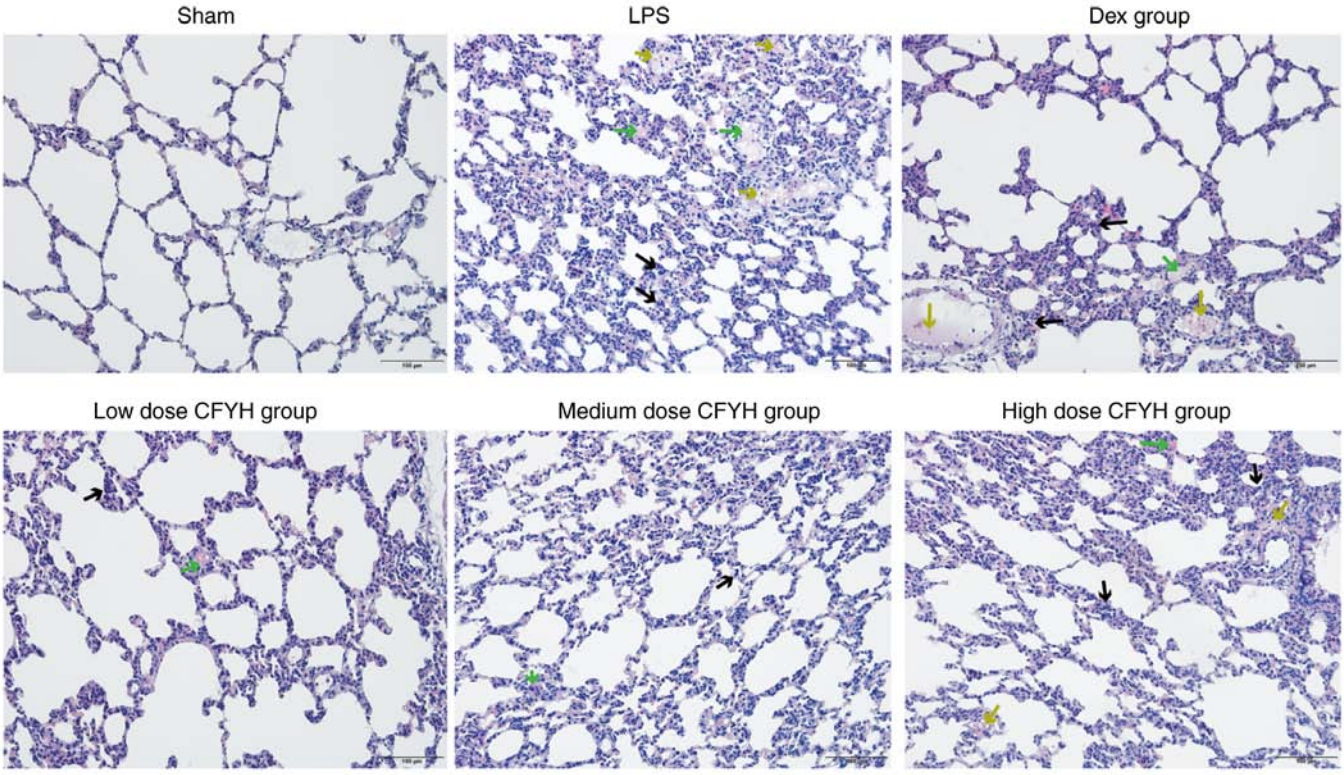

Figure 2. H&E staining of lung tissues from the Sham, LPS, Dex, low dose CFYH group, medium dose CFYH group, and high dose CFYH group. Green arrows show inflammatory exudates; yellow arrows show clear hemorrhaging; black arrows show inflammatory infiltration. CFYH, Chuanfangyihao; H&E, hematoxylin and eosin; Dex, Dexamethasone group; LPS, lipopolysaccharide group.

Effects of CFYH on the death pattern of lung cells in ALI rats

CFYH promotes autophagy in LPS-induced ALI. Western blotting was performed to detect AMPK, mTOR, phospho-AMPK, and phospho-mTOR (Fig. 5B). The phospho-AMPK/AMPK ratio was noticeably higher in the low dose CFYH group than in the LPS group. The phospho-mTOR/mTOR expression ratio was lower in the LPS group than in the sham group. Following pretreatment with CFYH and Dex, the phospho-mTOR/mTOR ratio decreased. The PCR results for AMPK and mTOR mRNA were consistent with those of western blotting (Fig. 6A-D).

The expression levels of LC3-II/I, Beclin-1, and P62 were detected using western blotting (Fig. 5B). The results showed that the LC3-II/I ratios of the CFYH and Dex groups were markedly higher than those of the LPS group, and the CFYH low dose group was higher than in the Dex group. Similarly, Beclin-1 protein expression levels were significantly higher in the low and medium-dose CFYH groups than in the LPS group. The expression trends of P62 at the protein level in the LPS group were reversed by CFYH and Dex, particularly in the low-dose CFYH group (Fig. 6E-G). Immunohistochemical analysis showed that the average optical density of Beclin-1 was higher in the low-dose CFYH group than in the LPS group (Fig. 7A and C). These results indicated that CFYH enhanced autophagy in LPS-induced lung injury.

CFYH inhibits apoptosis in the LPS-induced ALI rat model. To elucidate the relationship between LPS exposure and apoptosis, the expression of apoptosis-related proteins was determined. Compared to the LPS group, the expression levels of Bax protein in the low and medium-dose CFYH groups were markedly reduced. LPS exposure led to a notable increase in the expression of Caspase-3 at the protein level, and this increased expression of caspase-3 was inhibited by pretreatment with CFYH and Dex, especially by the low-dose CFYH group. The expression levels of Bcl-2 protein in the low and medium-dose CFYH and Dex groups were notably higher than those in the LPS group (Figs. 5B and 6H-J). These results suggested that CFYH suppressed apoptosis in LPS-triggered lung injury.

CFYH attenuates pyroptosis of LPS-induced ALI. Pyroptosis mediated LPS-induced pulmonary dysfunction. The protein expression of GSDMD-NT and Caspase-1 was examined by western blotting (Fig. 5B). These results suggest that the protein expression levels of GSDMD-NT and Caspase-1 in the lung tissues of the LPS group were markedly increased. The expression levels of GSDMD-NT were markedly reduced in the low and medium-dose CFYH and Dex groups. Additionally, the expression levels of Caspase-1 protein in the low and medium-dose CFYH groups were significantly downregulated (Fig. 6K and L). Immunohistochemical analysis was performed to detect NLRP3 expression. The mean optical density of NLRP3 was lower in the low and medium-dose CFYH groups than in the LPS group (Fig. 7B and C).

When a cell undergoes pyroptosis, the cell membrane is ruptured, and LDH is released extracellularly. ELISA was used to detect LDH levels, and the results showed that the LDH content in the CFYH group was notably lower than that in the LPS group (Fig. 6M). Furthermore, the low and medium-dose CFYH groups and Dex group reversed the effects of the LPS

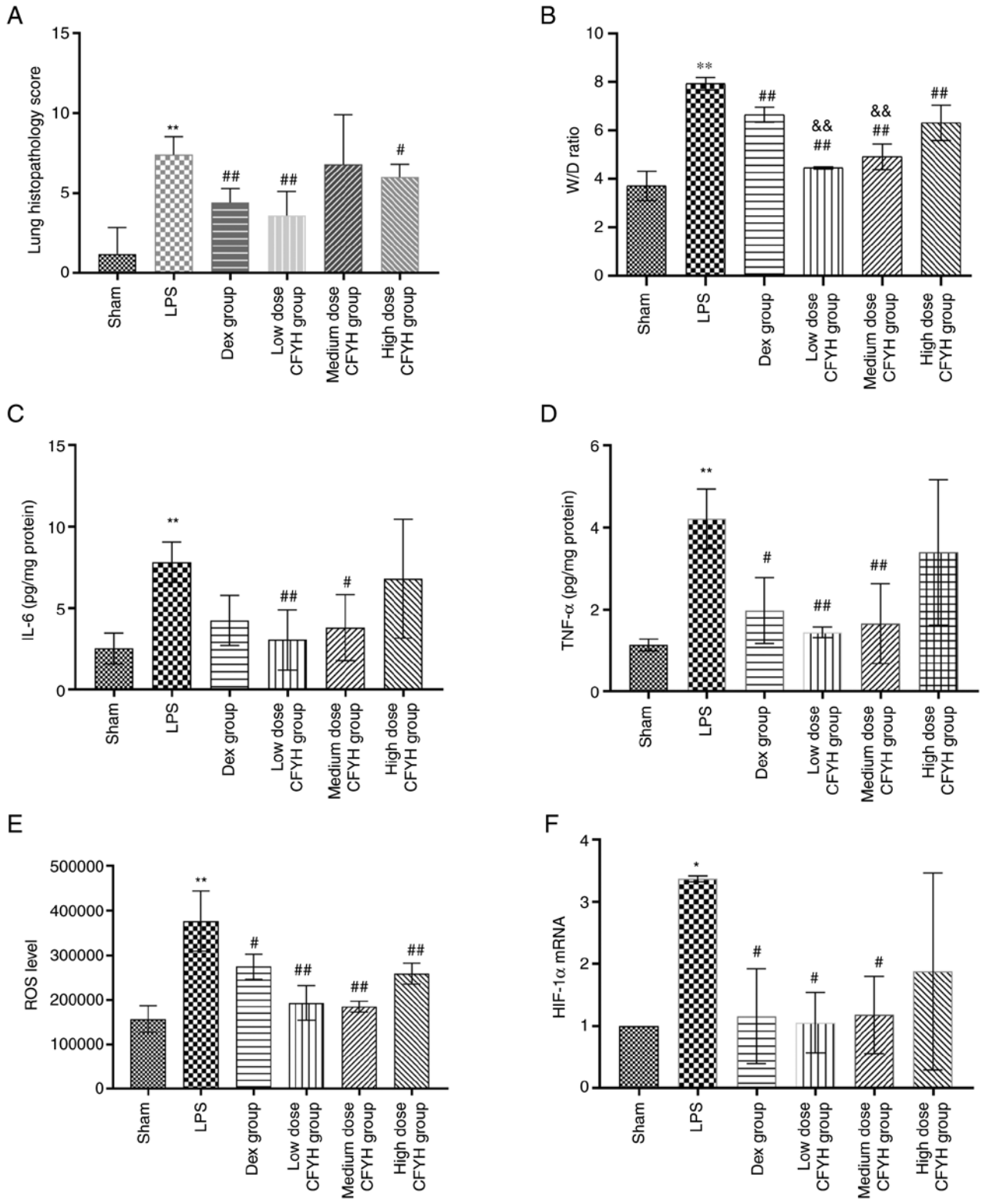

Figure 3. Analysis of pathological score, W/D, IL-6, TNF-α, ROS, and HIF-1α. (A) Pathological score of lung tissue. (B) W/D weight ratio of lung tissue. (C and D) IL-6 and TNF-α levels were determined by ELISA. (E) ROS levels were determined by flow cytometry assay. (F) HIF-1α levels were determined by quantitative PCR. *P<0.05, **P<0.01 vs. sham group; $^{\#}$P<0.05, $^{\#\#}$P<0.01 vs. LPS group; $^{\&\&}$P<0.01 vs. Dex group. W/D: ratio of wet weight to dry weight of lung tissue; ROS, reactive oxygen species.

group on IL-18 and IL-1β (Fig. 6N and O). These results indicate that CFYH alleviated pyroptosis.

Taken together, these results suggest that CFYH attenuated LPS-induced ALI in rats by regulating autophagy and repressing apoptosis and pyroptosis.

Discussion

In the present study, the potential pharmacological mechanism of CFYH in the management of ALI was investigated. The results revealed that CFYH effectively attenuated

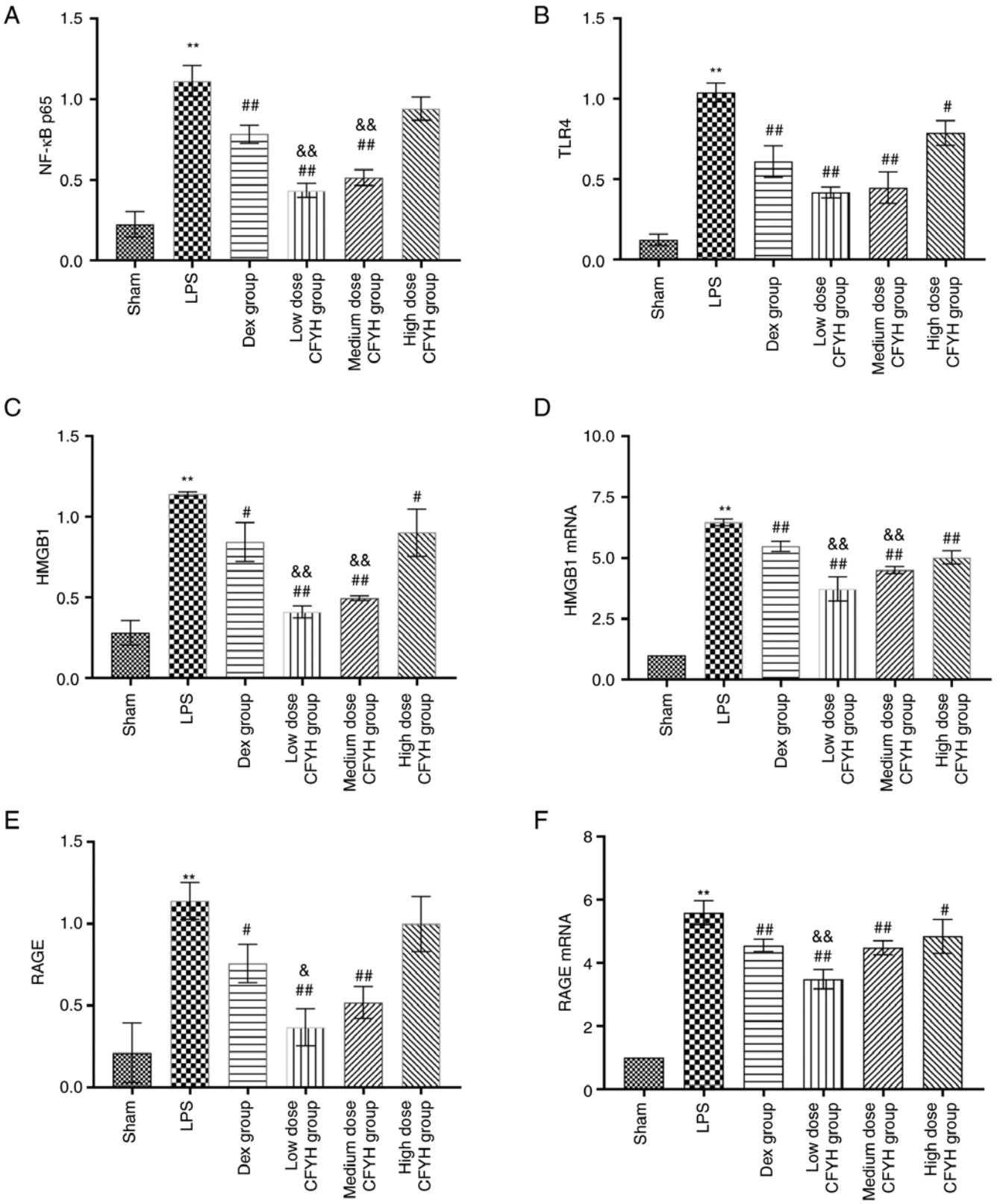

Figure 4. (A) NF-κB P65, (B) TLR4, and (C) HMGB1 protein expression levels were determined by western blotting. (D) HMGB1 mRNA expression levels were determined by PCR. (E) RAGE protein expression levels were determined by western blotting. (F) RAGE mRNA expression levels were determined by PCR. **P<0.01, ***P<0.001 vs. sham group; $^{\#}$P<0.05, $^{\#\#}$P<0.01 vs. LPS group; $^{\&}$P<0.05, $^{\&\&}$P<0.01vs. Dex group.

histopathological damage in a rat model of ALI induced using LPS while inhibiting apoptosis, pyroptosis, and inflammation.

ALI/ARDS is one of the leading causes of death in severe clinical cases of lung disease, characterized by its rapid onset and high fatality rate (24). Its impact is extensive and far-reaching (25), imposing a substantial economic burden on individuals and society. Moreover, it severely impairs the quality of life of patients, with lasting effects persisting

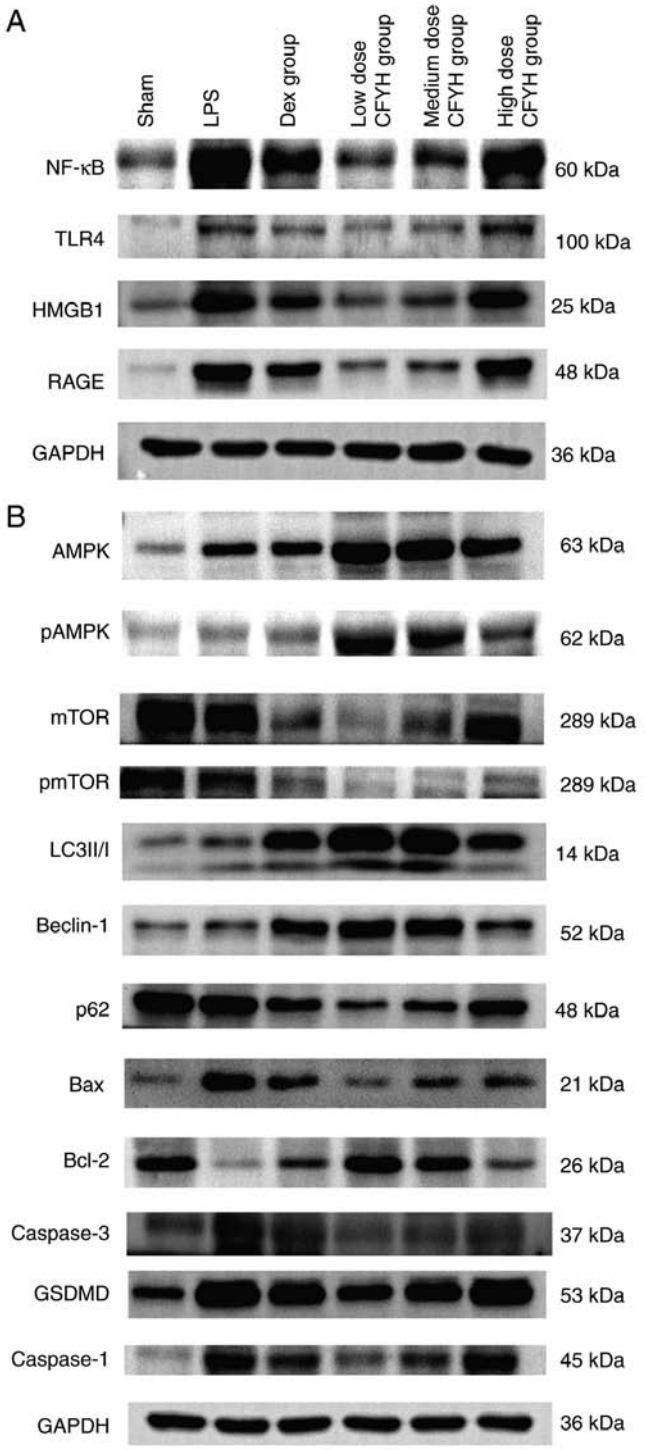

Figure 5. Western blotting analysis. (A) Western blotting analysis of NF-κB P65, TLR4, HMGB1 and RAGE expression levels. (B) Western blotting analysis of p-AMPK/AMPK, p-mTOR/mTOR, LC3-II/I, Beclin-1, P62, Bax, Caspase-3, Bcl-2, GSDMD-NT, Caspase-1, and NLRP3 expression levels. p, phosphorylated; LC3, microtubule-associated protein 1 light chain 3; HMGB1, high mobility group box 1; RAGE, receptor for advanced glycation end products; NLRP3, NOD-like receptor thermal protein domain associated protein 3; GSDMD-NT, gasdermin D N-terminal.

for up to 5 years after recovery (26). Unfortunately, there is currently no specific treatment available for this disease in the clinical practice (27). Therefore, effective prevention of ALI in its early stages and halting its progression to ARDS remain critical challenges that demand urgent attention (28).

In recent years, the application of TCM preparations and extracts for the prevention and treatment of ALI has garnered increasing attention from scholars (29). However, the chemical composition of TCM is complex, and not all compounds have pharmacological activity. This complexity poses a challenge to comprehensively studying the potential mechanism of Chinese medicinal formulations (30). The pathogenesis of ALI is intricate, and a single drug cannot achieve the expected therapeutic effect. TCM formulations can exert therapeutic effects through the synergistic actions of various pharmacologically active compounds (31). Through experimental verification, it was systematically elucidated the possible pharmacological mechanism of CFYH against ALI in the present study.

CFYH is derived from the classical, TCM prescriptions, Zhenwu concoction, and Buyanghuanwu concoction. Studies have demonstrated that Zhenwu concoction protects mitochondrial function and attenuates apoptosis (32,33). It has also shown potential in alleviating symptoms and promoting heart pulmonary function in patients with acute-stage chronic pulmonary heart disease (34). Buyanghuanwu concoction diminished the generation of Keap1, upregulated Nrf2 expression, and promoted the expression of HO-1 in a bleomycin-induced model (35). CFYH may be a promising method for managing lung disorders in clinical practice due it favorable efficacy (13,14), and the favorable safety profile of CHYF is also a major advantage. The combination of each Chinese medicine is performed in line with the composition norms of Chinese medicine formulas (36), and the dosages of the medicines in CFYH are in agreement with the standards of the safe use of TCM (37). Thus far, no safety risks have been found in patients taking CFYH. However, Chinese medicines often have a poor taste, and certain people who are not accustomed to the taste of Chinese medicines may find CFYH difficult to swallow.

The results of the present study provide a basis for experiments to verify the role of CFYH in LPS-induced ALI. There are several pathogenic factors that can lead to the development of ALI/ARDS, among which gram-negative bacterial infection-induced ALI accounts for a marked proportion (38). LPS, a glycolipid complex, is present in the cell wall of gram-negative bacteria. LPS activates mononuclear macrophages and induces the synthesis and release of pro-inflammatory cytokines, chemokines, growth factors, and a variety of other factors (39). The major toxicity centers and bioactive parts of LPS are highly conserved and non-species specific, thus the toxic effects of LPS produced by different strains are similar (40). Consequently, LPS is often used to construct animal models of ALI, as the inflammatory injury induced by LPS in the body is similar to that of a real infection caused by gram-negative bacteria (41). In the LPS-induced ALI rats, massive inflammatory cell infiltration, alveolar space, interstitial edema, red blood cell leakage, alveolar wall congestion, and alveolar wall thickening were observed, indicating the successful establishment of the model. Moreover, the CFYH group alleviated the histopathological damage of the rat lung tissues to varying degrees.

Excessive production of inflammatory cytokines and oxygen free radicals are two major contributors to LPS-induced ALI. Several inflammatory mediators accumulate in the lungs after LPS stimulation (42). As a common DAMP, HMGB1 can

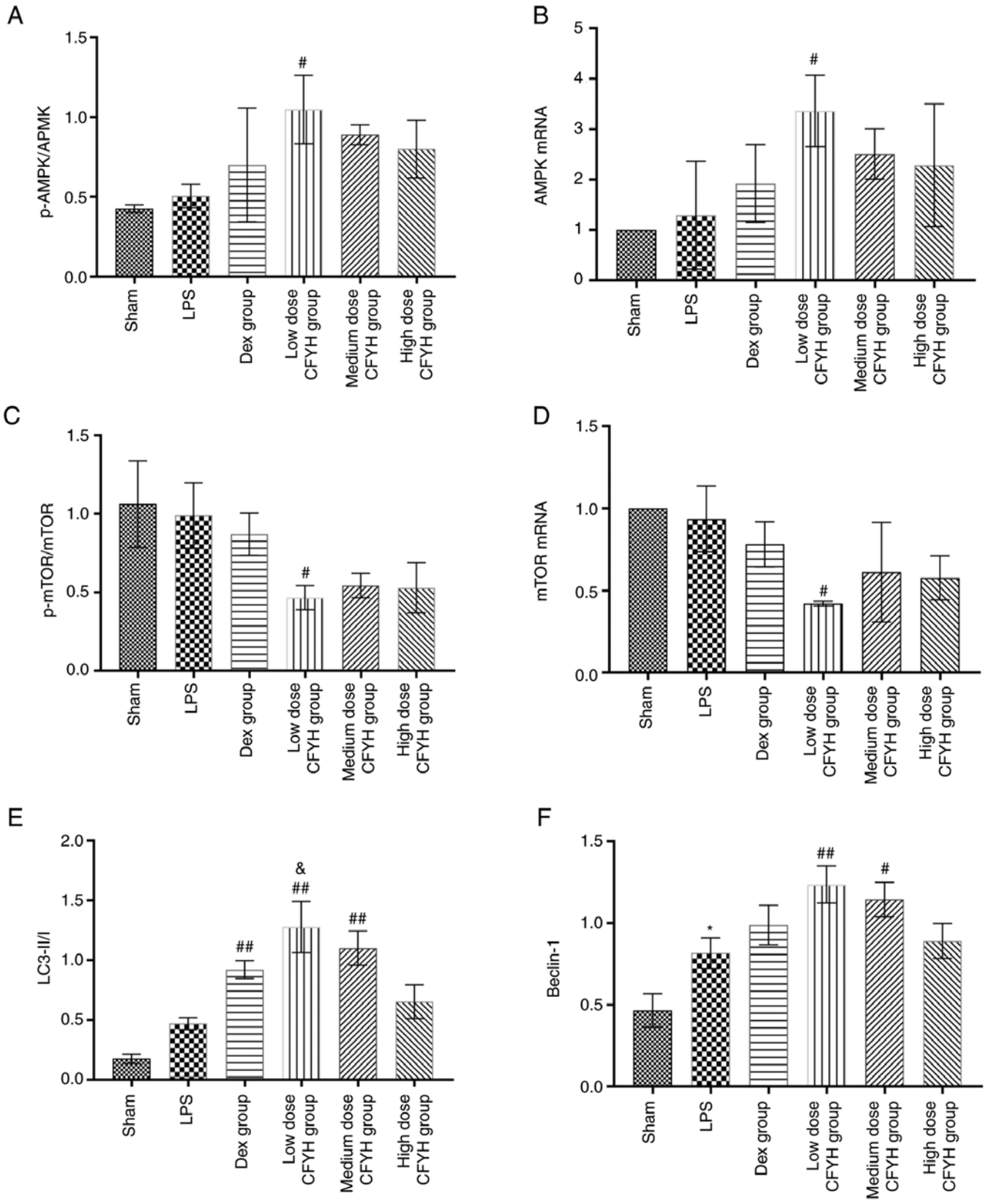

Figure 6. Continued.

amplify the inflammatory cascade, and it is also an important late inflammatory factor in the inflammatory response of ALI/ARDS, and its synthesis and release directly affect the occurrence and development of ALI/ARDS (43,44). Extracellular HMGB1 binds to receptors such as RAGE and TLR4 on the cell surface, activating several downstream inflammatory signaling pathways and inducing inflammatory mediators such as NF-κB, IL-6, and TNF-α, thus enhancing the inflammatory response in lung tissues. This interaction between HMGB1 and inflammatory cytokines creates a

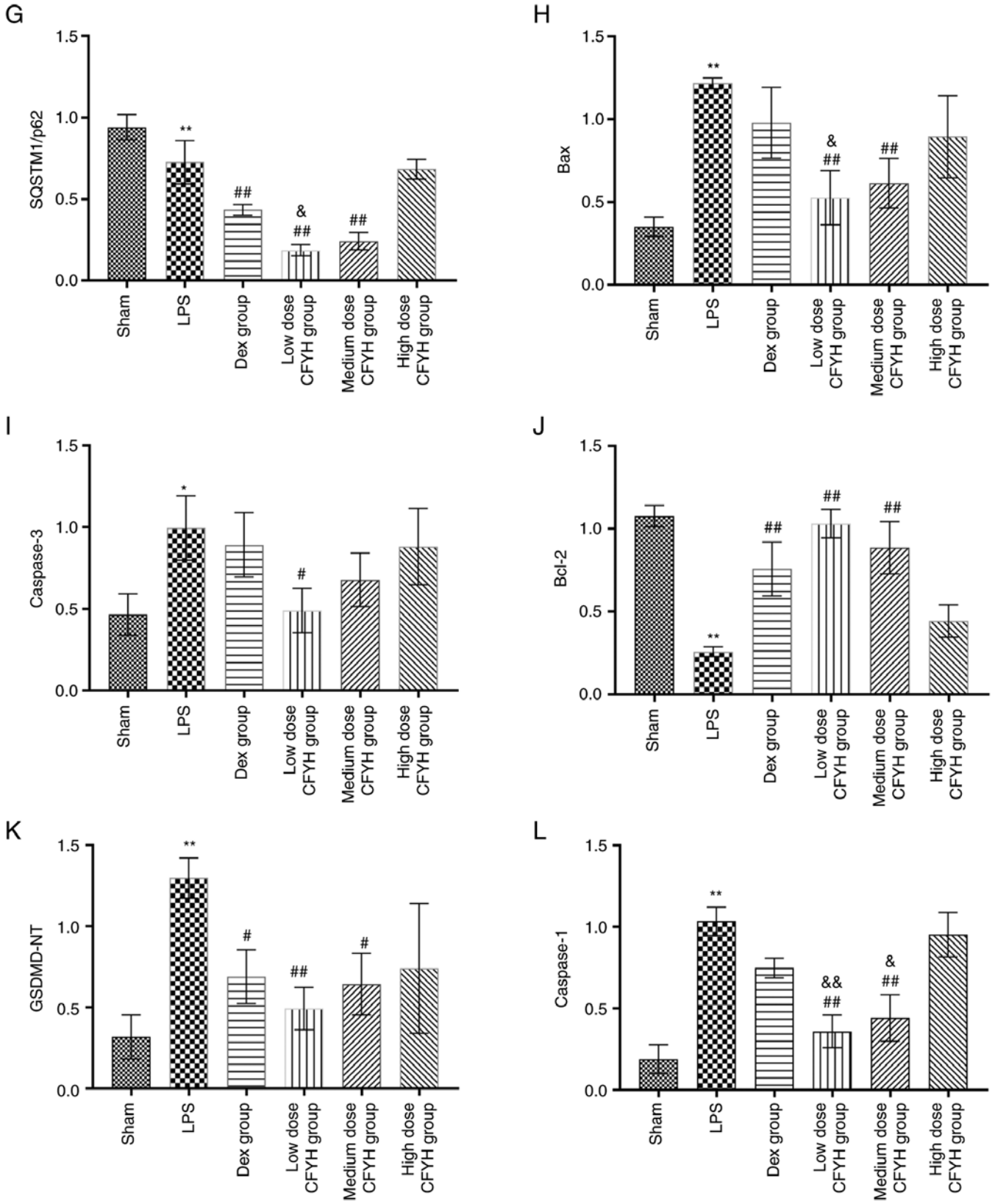

Figure 6. Continued.

vicious cycle, aggravating the degree of respiratory dysfunction and lung injury.

LPS-induced inflammation is often accompanied by hypoxia (45). A continuous supply of ATP is key to maintaining physiological activities. ATP synthesis is primarily performed by mitochondria (46), which produce large quantities of ROS during hypoxia. ROS damage of pulmonary microvascular endothelial cells and epithelial cells, increases pulmonary vascular permeability, and leads to the formation of pulmonary edema (47-49). Both hypoxia and inflammation can

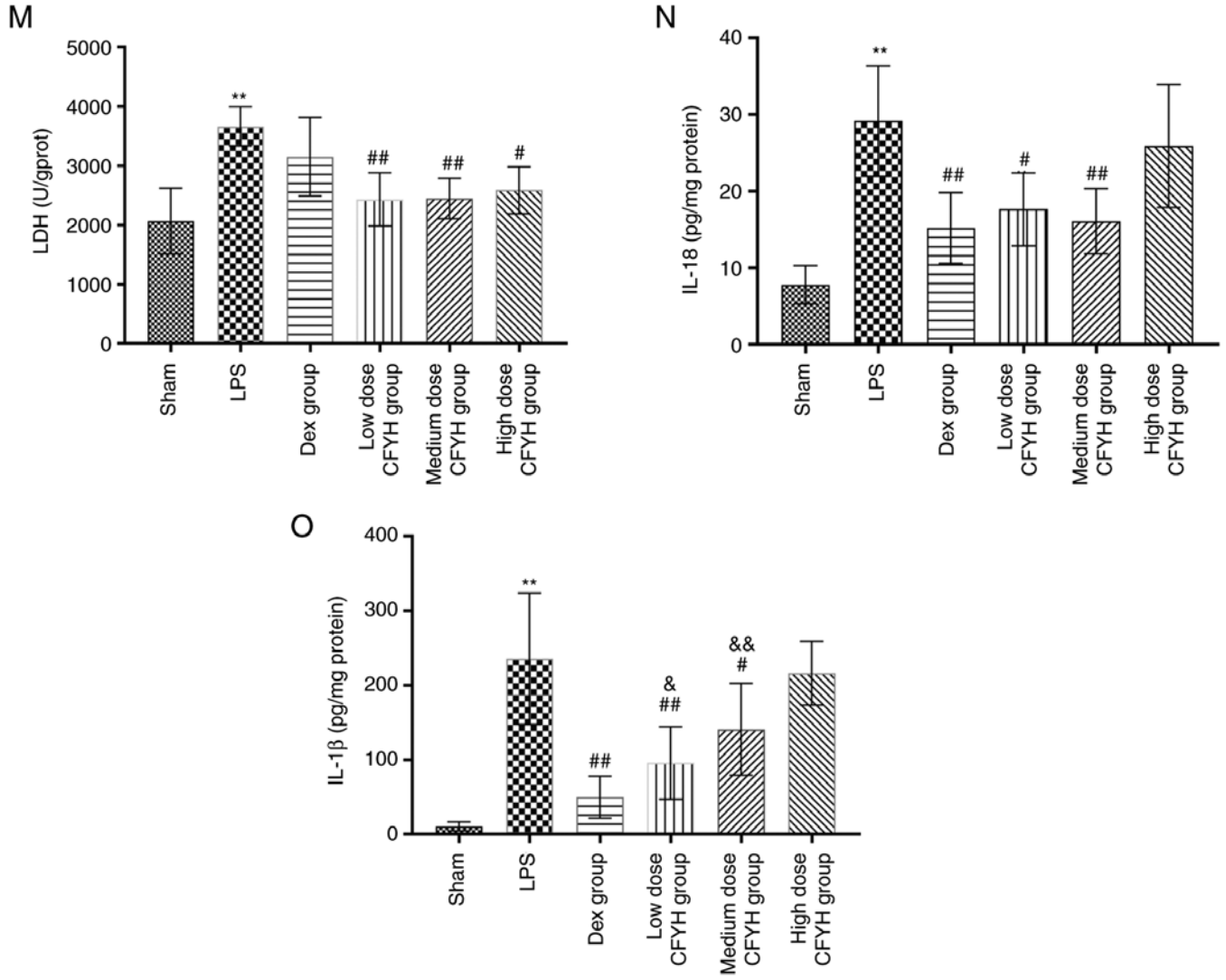

Figure 6. (A) The levels of p-AMPK/AMPK were determined by western blotting; (B) The mRNA expression levels of AMPK were determined by PCR. (C) The levels of p-mTOR/mTOR were determined by western blotting. (D) The mRNA expression levels of mTOR were determined by PCR. The levels of (E) LC3-II/I, (F) Beclin-1, (G) P62, (H) Bax, (I) Caspase-3, (J) Bcl-2, (K) GSDMD-NT and (L) Caspase-1 were determined by western blotting. The levels of (M) LDH, (N) IL-18 and (O) IL-1β were determined by ELISA. *P<0.05, **P<0.01 vs. sham group; $^{\#}$P<0.05, $^{\#\#}$P<0.01 vs. LPS group; $^{\&}$P<0.05, $^{\&\&}$P<0.01 vs. Dex group. P, phosphorylated; LC3, microtubule-associated protein 1 light chain 3; HMGB1, high mobility group box 1; RAGE, receptor for advanced glycation end products; NLRP3, NOD-like receptor thermal protein domain associated protein 3; GSDMD-NT, gasdermin D N-terminal.

stimulate the upregulation of HIF-1α (50,51). HIF-1α is also an important inflammatory regulator that promotes the release of various pro-inflammatory factors, such as TNF-α, IL-1β, and IL-6, which further aggravates the pulmonary inflammatory response through their interactions (52,53). These results show that HMGB1 and RAGE at the protein and mRNA level, IL-6, TNF-α, NF-κB P65, TLR4, and ROS levels were significantly increased following LPS induction. Interestingly, these effects were reversed by CFYH treatment. These results suggest that CFYH protects against ALI through its anti-inflammatory and antioxidant effects.

Programmed cell death is often associated with inflammation, and autophagy, apoptosis, and pyroptosis are involved in the occurrence and development of LPS-related ALI (38,54-59,60). The entire autophagy process is regulated by >30 autophagy-related genes (Atgs) (61). AMPK acts as an energy metabolism switch and activates autophagy by inhibiting mTOR phosphorylation (62,63). Microtubule-associated protein 1 light chain 3 (LC3) is an autophagy marker that is responsible for regulating the elongation and extension of autophagosome membranes, and the ratio of LC3-II/I can be used to estimate the levels of autophagy (64-66). The Atg Beclin-1 interferes with the formation of autophagosomes at different stages, and the p62 protein is primarily responsible for the degradation of autophagy substrates (67,68). When autophagy occurs, LC3 is transformed from type I to type II, beclin-1 expression level is increased, and P62 is gradually degraded (69). The results of the present study showed that AMPK, LC3-II/I, and Beclin-1 in lung tissues of rats in the LPS group were increased and significantly decreased after CFYH intervention. The expression levels of P62 and mTOR in the LPS group decreased, and CFYH had the opposite effect. These results suggest that CFYH enhances autophagy.

Bcl-2 and the Caspase families of proteins play important roles in the regulation of the apoptosis pathway (70). Bax and Bcl-2 are a pair of positive and negative regulators, with Bax

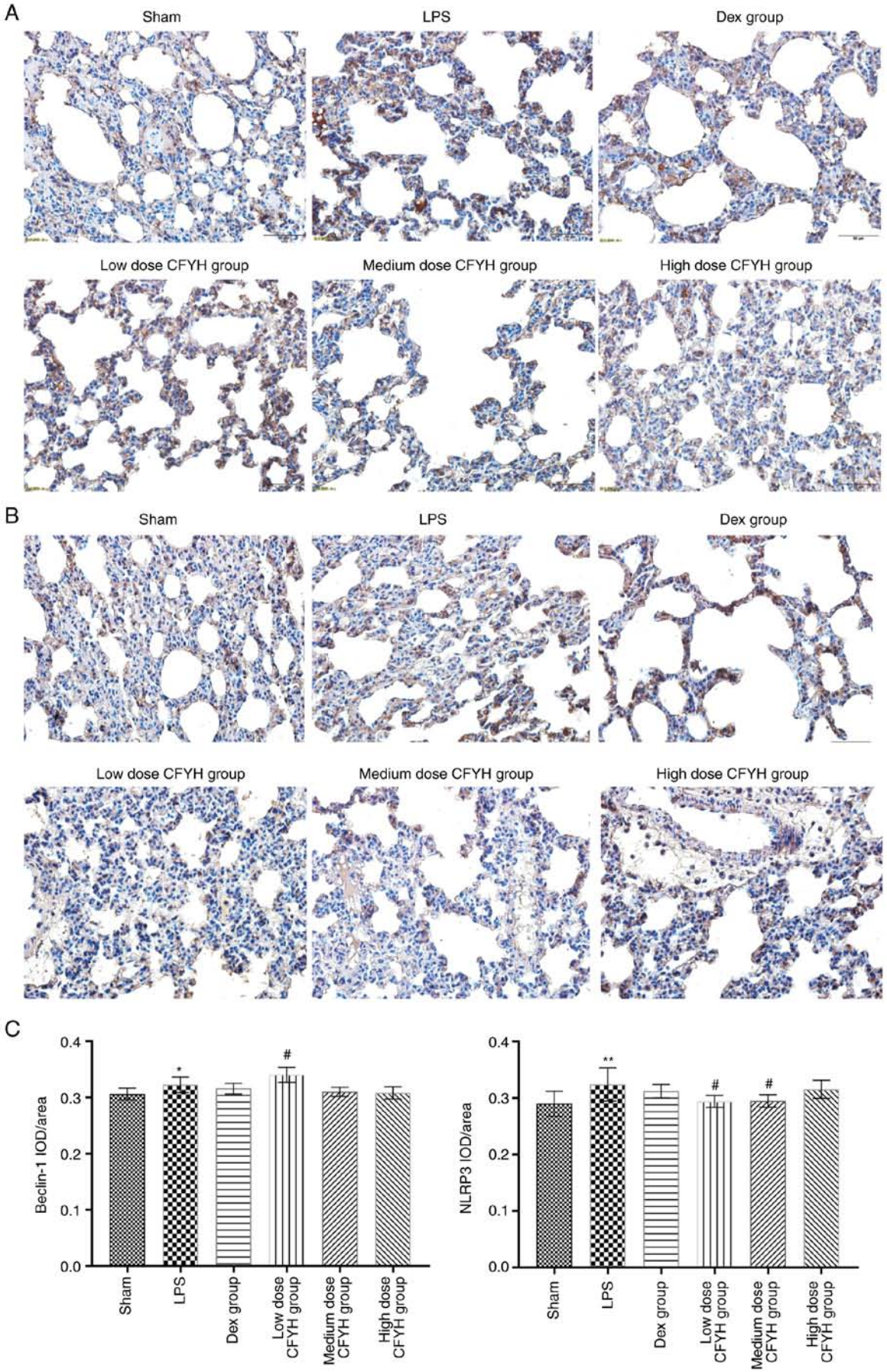

Figure 7. Results of immunohistochemistry analysis. (A) Immunohistochemistry analysis of Beclin-1 in the Sham, LPS, Dex, and low, medium, and high-dose CFYH groups. (B) Immunohistochemistry analysis of NLRP-3 in the Sham, LPS, Dex, and low, medium, and high-dose CFYH groups. (C) The levels of Beclin-1 and NLRP3 were detected by immunohistochemical analysis. $^{*}P<0.05$, $^{**}P<0.01$ vs. sham group; $^{\#}P<0.05$, $^{\#\#\#}P<0.001$ vs. LPS group. CFYH, Chuanfangyihao; Dex, Dexamethasone group; LPS, lipopolysaccharide group.

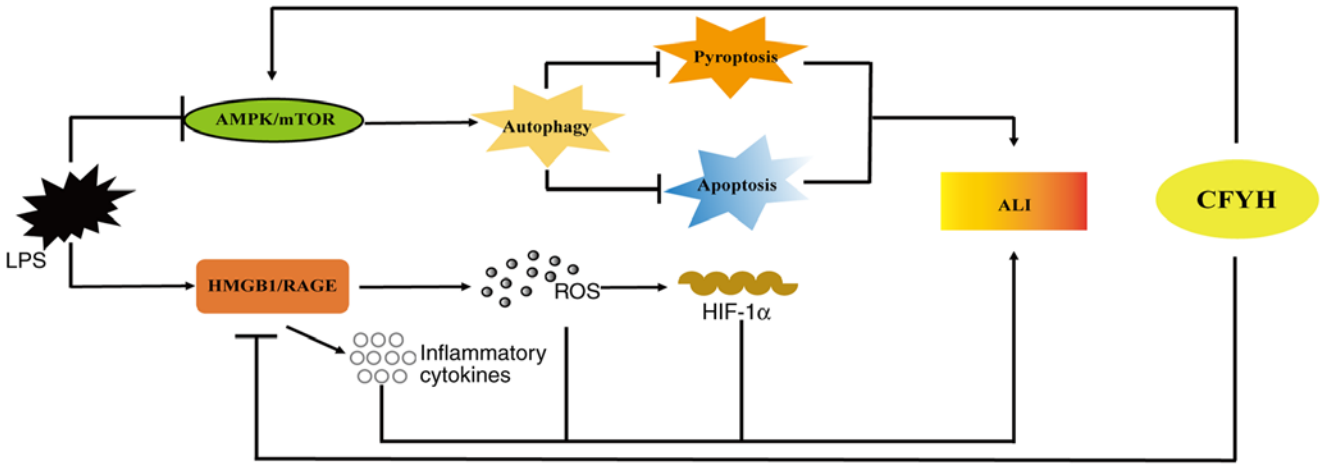

Figure 8. The protective effect of CFYH on LPS-induced lung injury and the underlying mechanism of action. CFYH pretreatment significantly protected against LPS-induced lung injury through the reduction of oxidative stress and inflammation and altering cell death patterns, mediated by the activation of the AMPK/mTOR and HMGB1/RAGE signaling pathways.

promoting apoptosis and Bcl-2 preventing apoptosis (71). Caspase-3 is located downstream of different apoptosis pathways and is a key executioner of apoptosis, and its cleavage indicates a commitment to apoptosis (72). The experimental results of the present study showed that the expression levels of Bax and Caspase-3 were significantly increased in the LPS group, which could not be reversed by Dex, but was reversed by CFYH. After CFYH intervention, Bcl-2 protein levels were significantly higher than those in the LPS group. These results indicate that CFYH inhibits apoptosis.

Pyroptosis, also known as cell inflammatory necrosis, is induced by the inflammasome and initiates through gasdermin-D activation by the inflammatory caspase family, which causes cell membrane perforation, cell lysis, and the release of cellular contents, such as activated IL-1β and IL-18. IL-1β and IL-18 inflammatory factors produce pro-inflammatory signals, which amplify the inflammatory response and lead to 'pathological suicide' of the cell (73). The occurrence, development, and severity of ALI depend on this process (74-78). The results of the present study showed that the levels of key pyroptosis proteins in the LPS group were significantly higher than those in the sham group. After CFYH intervention, the expression of all the measured proteins was reduced to varying degrees. Although none of the indicators showed obvious dose dependence in the low, medium, and high-dose CFYH groups, as a whole, CFYH blocked pyroptosis in rats with ALI.

The functional relationship between autophagy, apoptosis, and pyroptosis is complicated and subtle (79,80). Studies have shown that when cells are subjected to a level of low environmental pressures (slight or early inflammation), they initiate autophagic mechanisms to overcome the pressure, and autophagy increases sharply. This increase in autophagy inhibits the apoptosis and pyroptosis of cells. Conversely, under severe inflammatory conditions, the body initiates the mechanism of apoptosis and pyroptosis, leading to further damage (81-86). The AMPK/mTOR signaling pathway, as an important signaling pathway regulating the autophagy-apoptosis-pyroptosis balance, has been shown to play a key role in the improvement of ALI.

The design of the present study was based on the concept of prevention (87,88), and the purpose was to observe whether Chinese medicines had a therapeutic effect for the treatment of ALI, after reaching its requisite blood concentration in animals. Future studies will focus on the idea of developing and administering TCM after therapeutic modeling.

In conclusion, it was shown that CFYH exhibited a favorable effect against LPS-induced ALI. This protective effect may be mediated by downregulating the HMGB1/RAGE signaling pathway, reducing the release of inflammatory factors, inhibiting oxidative stress, activating the AMPK/mTOR signaling pathway, enhancing lung cell autophagy, and inhibiting lung cell pyroptosis and apoptosis (Fig. 8). These results suggest that CFYH has anti-inflammatory, anti-stress, and anti-apoptosis properties. The present study provides a theoretical basis for the clinical application of CFYH in the treatment of ALI. However, an in-depth study of these mechanisms requires further investigation.

Acknowledgements

Not applicable.

Funding

This study was funded by the Sichuan Provincial Administration of Traditional Chinese Medicine (grant no. CKY2021155).

Availability of data and materials

All data generated or analyzed during this study are included in this published article.

Authors' contributions

HF, XL, WT, and XH designed the study. HF, XL, and WT performed the experiments. HF and XL were responsible for primary data generation, analysis, and writing of the manuscript. WT and XH revised the manuscript. All authors have

read and approved the final manuscript. HF, XL and XH confirm the authenticity of all the raw data.

Ethics approval and consent to participate

All experiments were performed in accordance with the National Institutes of Health Guide for the Care and Use of Laboratory Animals and were approved by the ethical committee for the experimental use of animals at Sichuan Academy of Traditional Chinese Medicine [approval no. SYLL(2022)-039].

Patient consent for publication

Not applicable.

Competing interests

The authors declare that they have no competing interests.

References

1. Monsel A, Zhu YG, Gudapati V, Lim H and Lee JW: Mesenchymal stem cell derived secretome and extracellular vesicles for acute lung injury and other inflammatory lung diseases. Expert Opin Biol Ther 16: 859-871, 2016.
2. Wang LP and Tang XQ: Study on early warning signals of acute lung injury. Life Sci Res 25: 532-539, 2021.
3. Zambon M and Vincent JL: Mortality rates for patients with acute lung injury/ARDS have decreased over time. Chest 133: 1120-1127, 2008.
4. Matthay MA, Zemans RL, Zimmerman GA, Arabi YM, Beitler JR, Mercat A, Herridge M, Randolph AG and Calfee CS: Acute respiratory distress syndrome. Nat Rev Dis Primers 5: 18, 2019.
5. Al Masry A, Boules ML, Boules NS and Ebied RS: Optimal method for selecting PEEP level in ALI/ARDS patients under mechanical ventilation. J Egypt Soc Parasitol 42: 359-372, 2012.
6. Fan E, Del Sorbo L, Goligher EC, Hodgson CL, Munshi L, Walkey AJ, Adhikari NKJ, Amato MBP, Branson R, Brower RG, *et al*: An official American thoracic society/European society of intensive care medicine/society of critical care medicine clinical practice guideline: Mechanical ventilation in adult patients with acute respiratory distress syndrome. Am J Respir Crit Care Med 195: 1253-1263, 2017.
7. Duggal A, Rezoagli E, Pham T, McNicholas BA, Fan E, Bellani G, Rubenfeld G, Pesenti AM and Laffey JG; LUNG SAFE Investigators and the ESICM Trials Group: Patterns of use of adjunctive therapies in patients with early moderate to severe ARDS: Insights from the LUNG SAFE study. Chest 157: 1497-1505, 2020.
8. Rosenberg OA: Pulmonary surfactant preparations and surfactant therapy for ARDS in surgical intensive care (a literature review). Creat Surg Oncol 9: 50-65, 2019.
9. Badet M, Bayle F, Richard JC and Guérin C: Comparison of optimal positive end-expiratory pressure and recruitment maneuvers during lung-protective mechanical ventilation in patients with acute lung injury/acute respiratory distress syndrome. Respir Care 54: 847-854, 2009.
10. Fukuda Y: Acute lung injury/acute respiratory distress syndrome: progress in diagnosis and treatment. Topics: I. Pathogenesis and pathophysiology: 4. Pathophysiology and histopathology of ALI/ARDS. Nihon Naika Gakkai Zasshi 100: 1536-1540, 2011 (In Japanese).
11. Zhang X, Zheng J, Yan Y, Ruan Z, Su Y, Wang J, Huang H, Zhang Y, Wang W, Gao J, *et al*: Angiotensin-converting enzyme 2 regulates autophagy in acute lung injury through AMPK/mTOR signaling. Arch Biochem Biophys 672: 108061, 2019.
12. Su JS, Liu ES and Zhao XM: Advances in the treatment of acute lung injury/acute respiratory distress syndrome with traditional chinese medicine. Jilin J Tradit Chin Med: 37, 2019 (In Chinese).
13. Wang SB: Clinical characteristics and risk factors of severe pneumonia in 165 cases of novel coronavirus pneumonia. Chengdu University of TCM, 2021 (In Chinese).
14. Liu M: Effect of chuanfang no: L exposure on COVID-19 a retrospective cohort study based on propensity score matching. Chengdu University of TCM, 2021 (In Chinese).
15. Huang JH, Huang XH, Chen ZY, Zheng QS and Sun RY: Dose conversion among different animals and healthy volunteers in pharmacological study. Chin J Clin Pharmacol Ther 9: 1069-1072, 2004.
16. Arck PC: When 3 Rs meet a forth R: Replacement, reduction and refinement of animals in research on reproduction. J Reprod Immunol 132: 54-59, 2019.
17. Kilkenny C, Browne W, Cuthill IC, Emerson M and Altman DG; NC3Rs Reporting Guidelines Working Group: Animal research: Reporting in vivo experiments: the ARRIVE guidelines. Br J Pharmacol 160: 1577-1579, 2010.
18. Wang GQ: The effect and mechanism of Lianggesan on fluid transportion in endotoxin acute lung injury tissue. So Med Univ, 2014 (In Chinese).
19. Wang XH, Yan SG, Hui Y, Shi J and Li JT: Mechanism of ephedrae Herba-rhei Radix et Rhizoma drug pair on treating acute lung injury based on alveolar macrophage M2 polarization. Chin Tradit Herbal Drugs 53: 2715-2722, 2022 (In Chinese).
20. Pei CX, Wang XM, Wu YC, Wang ZX, Huang DM, Yang Q, *et al*: Studies on mechanism of platycodin D inhibiting apoptosis and protecting acute lung injury via Bax/bcl-2/caspase-3 signaling pathway. Modernization Tradit Chin Med Materia Medica-World Sci and Tech 23: 3551-3558, 2021 (In Chinese).
21. Mikawa K, Nishina K, Takao Y and Obara H: ONO-1714, a nitric oxide synthase inhibitor, attenuates endotoxin-induced acute lung injury in rabbits. Anesth Analg 97: 1751-1755, 2003.
22. Livak KJ and Schmittgen TD: Analysis of relative gene expression data using real-time quantitative PCR and the 2(-Delta Delta C(T)) method. Methods 25: 402-408, 2001.
23. Cumming G, Fidler F and Vaux DL: Error bars in experimental biology. J Cell Biol 177: 7-11, 2007.
24. Huang X, Xiu H, Zhang S and Zhang G: The role of macrophages in the pathogenesis of ALI/ARDS. Mediators Inflamm 2018: 1264913, 2018.
25. Janz DR and Ware LB: Biomarkers of ALI/ARDS: Pathogenesis, discovery, and relevance to clinical trials. Semin Respir Crit Care Med 34: 537-548, 2013.
26. Bos LD, Martin-Loeches I and Schultz MJ: ARDS: Challenges in patient care and frontiers in research. Eur Respir Rev 27: 170107, 2018.
27. Spieth PM and Zhang H: Pharmacological therapies for acute respiratory distress syndrome. Curr Opin Crit Care 20: 113-121, 2014.
28. Zhao R, Wang B, Wang D, Wu B, Ji P and Tan D: Oxyberberine prevented lipopolysaccharide-induced acute lung injury through inhibition of mitophagy. Oxid Med Cell Longev 2021: 6675264, 2021.
29. Yu WY, Gao CX, Zhang HH, Wu YG and Yu CH: Herbal active ingredients: potential for the prevention and treatment of acute lung injury. Biomed Res Int 2021: 5543185, 2021.
30. Hao X, Liu Y, Zhou P, Jiang Q, Yang Z, Xu M, Liu S, Zhang S and Wang Y: Integrating network pharmacology and experimental validation to investigate the mechanisms of huazhuojiedu decoction to treat chronic atrophic gastritis. Evid Based Complement Alternat Med 2020: 2638362, 2020.
31. Li C: Multi-compound pharmacokinetic research on Chinese herbal medicines: Approach and methodology. Zhongguo Zhong Yao Za Zhi 42: 607-617, 2017 (In Chinese).
32. Li Z, Li WJ, Shang XY and Yu KY: Effect of Zhenwu Decoction on myocardial mitochondrial damage and cardiomyocyte apoptosis in heart failure rats by SIRT1 signaling pathway. Chin Arch Tradit Chin Med 36: 1062-1067, 2018 (In Chinese).
33. Wang YH, Li WJ and Li Z: Effect of serum containing Zhenwu Decoction on cardiomyocyte apoptosis and Bcl-2 and Bax protein expression induced by isoproterenol in Rats. Liaoning J Trad Chin Med 45: 1305-1308+1346, 2018 (In Chinese).
34. Yang PQ, Li QY and Fang S: Effect of Zhenwu Decoction combined with Benazepril on the curative effect and cardiopulmonary function of chronic pulmonary heart disease in acute stage. J Emerg Trad Chin Med 31: 854-856, 2022 (In Chinese).
35. Zhang Z, Zhao S, Han YP, Jin F, Shang JR, Wang JP and Fang CY: Effect of Buyang Huanwu Decoction on Keap1/Nrf2/HO-1 antioxidant signaling pathway in rats with idiopathic pulmonary fibrosis. Chin J Exp Trad Med formula: 1-10 (In Chinese).
36. National Pharmacopoeia Commission, Pharmacopoeia of the People's Republic of China (2020 Edition), China Medical Sciences Press, 2020.

37. Gao XM: Traditional Chinese pharmacy. China Traditional Chinese Medicine Press, 2002-1.
38. Li H, Li Y, Song C, Hu Y, Dai M, Liu B and Pan P: Neutrophil extracellular traps augmented alveolar macrophage pyroptosis via AIM2 inflammasome activation in LPS-induced ALI/ARDS. J Inflamm Res 14: 4839-4858, 2021.
39. Song C, Li H, Li Y, Dai M, Zhang L, Liu S, Tan H, Deng P, Liu J, Mao Z, *et al*: NETs promote ALI/ARDS inflammation by regulating alveolar macrophage polarization. Exp Cell Res 382: 111486, 2019.
40. Chen H, Bai C and Wang X: The value of the lipopolysaccharide-induced acute lung injury model in respiratory medicine. Expert Rev Respir Med 4: 773-783, 2010.
41. Fujita M, Kuwano K, Kunitake R, Hagimoto N, Miyazaki H, Kaneko Y, Kawasaki M, Maeyama T and Hara N: Endothelial cell apoptosis in lipopolysaccharide-induced lung injury in mice. Int Arch Allergy Immunol 117: 202-208, 1998.
42. Fukatsu M, Ohkawara H, Wang X, Alkebsi L, Furukawa M, Mori H, Fukami M, Fukami SI, Sano T, Takahashi H, *et al*: The suppressive effects of Mer inhibition on inflammatory responses in the pathogenesis of LPS-induced ALI/ARDS. Sci Signal 15: eabd2533, 2022.
43. Li N, Geng C, Hou S, Fan H and Gong Y: Damage-associated molecular patterns and their signaling pathways in primary blast lung injury: New research progress and future directions. Int J Mol Sci 21: 6303, 2020.
44. Wang G, Han D, Zhang Y, Xie X, Wu Y, Li S and Li M: A novel hypothesis: Up-regulation of HO-1 by activation of PPARγ inhibits HMGB1-RAGE signaling pathway and ameliorates the development of ALI/ARDS. J Thorac Dis 5: 706-710, 2013.
45. Xu Y, Li J, Lin Z, Liang W, Qin L, Ding J, Chen S and Zhou L: Isorhamnetin alleviates airway inflammation by regulating the Nrf2/Keap1 pathway in a mouse model of COPD. Front Pharmacol 13: 860362, 2022.
46. Meyer A, Zoll J, Charles AL, Charloux A, de Blay F, Diemunsch P, Sibilia J, Piquard F and Geny B: Skeletal muscle mitochondrial dysfunction during chronic obstructive pulmonary disease: Central actor and therapeutic target. Exp Physiol 98: 1063-1078, 2013.
47. Bouitbir J, Charles AL, Echaniz-Laguna A, Kindo M, Daussin F, Auwerx J, Piquard F, Geny B and Zoll J: Opposite effects of statins on mitochondria of cardiac and skeletal muscles: A 'mitohormesis' mechanism involving reactive oxygen species and PGC-1. Eur Heart J 33: 1397-1407, 2012.
48. Yu J, Wang Y, Li Z, Dong S, Wang D, Gong L, Shi J, Zhang Y, Liu D and Mu R: Effect of heme oxygenase-1 on mitofusin-1 protein in LPS-induced ALI/ARDS in rats. Sci Rep 6: 36530, 2016.
49. Lee SY, Li MH, Shi LS, Chu H, Ho CW and Chang TC: Rhodiola crenulata extract alleviates hypoxic pulmonary edema in rats. Evid Based Complement Alternat Med 2013: 718739, 2013.
50. Balamurugan K: HIF-1 at the crossroads of hypoxia, inflammation, and cancer. Int J Cancer 138: 1058-1066, 2016.
51. Eltzschig HK and Carmeliet P: Hypoxia and inflammation. N Engl J Med 364: 656-665, 2011.
52. Devraj G, Beerlage C, Brüne B and Kempf VA: Hypoxia and HIF-1 activation in bacterial infections. Microbes Infect 19: 144-156, 2017.
53. Cummins EP, Keogh CE, Crean D and Taylor CT: The role of HIF in immunity and inflammation. Mol Aspects Med 47-48: 24-34, 2016.
54. Zhao J, Jiang P, Guo S, Schrodi SJ and He D: Apoptosis, autophagy, NETosis, necroptosis, and pyroptosis mediated programmed cell death as targets for innovative therapy in rheumatoid arthritis. Front Immunol 12: 809806, 2021.
55. Van Opdenbosch N and Lamkanfi M: Caspases in cell death, inflammation, and disease. Immunity 50: 1352-1364, 2019.
56. Kesavardhana S, Malireddi RKS and Kanneganti TD: Caspases in cell death, inflammation, and pyroptosis. Annu Rev Immunol 38: 567-595, 2020.
57. Liu X, Gao C, Wang Y, Niu L, Jiang S and Pan S: BMSC-derived exosomes ameliorate LPS-induced acute lung injury by miR-384-5p-controlled alveolar macrophage autophagy. Oxid Med Cell Longev 2021: 9973457, 2021.
58. Wu D, Zhang H, Wu Q, Li F, Wang Y, Liu S and Wang J: Sestrin 2 protects against LPS-induced acute lung injury by inducing mitophagy in alveolar macrophages. Life Sci 267: 118941, 2021.
59. Zhao X, Yu Z, Lv Z, Meng L, Xu J, Yuan S and Fu Z: Activation of alpha-7 nicotinic acetylcholine receptors (α7nAchR) promotes the protective autophagy in LPS-induced acute lung injury (ALI) in vitro and in vivo. Inflammation 42: 2236-2245, 2019.
60. Ning L, Wei W, Wenyang J, Rui X and Qing G: Cytosolic DNA-STING-NLRP3 axis is involved in murine acute lung injury induced by lipopolysaccharide. Clin Transl Med 10: e228, 2020.
61. Klionsky DJ, Codogno P, Cuervo AM, Deretic V, Elazar Z, Fueyo-Margareto J, Gewirtz DA, Kroemer G, Levine B, Mizushima N, *et al*: A comprehensive glossary of autophagy-related molecules and processes. Autophagy 6: 438-448, 2010.
62. Kim J, Kundu M, Viollet B and Guan KL: AMPK and mTOR regulate autophagy through direct phosphorylation of Ulk1. Nat Cell Biol 13: 132-141, 2011.
63. Alers S, Löffler AS, Wesselborg S and Stork B: Role of AMPK-mTOR-Ulk1/2 in the regulation of autophagy: Cross talk, shortcuts, and feedbacks. Mol Cell Biol 32: 2-11, 2012.
64. Tanida I, Ueno T and Kominami E: LC3 and autophagy. Methods Mol Biol 445: 77-88, 2008.
65. Mizushima N and Levine B: Autophagy in human diseases. N Engl J Med 383: 1564-1576, 2020.
66. Qu L, Chen C, He W, Chen Y, Li Y, Wen Y, Zhou S, Jiang Y, Yang X, Zhang R and Shen L: Glycyrrhizic acid ameliorates LPS-induced acute lung injury by regulating autophagy through the PI3K/AKT/mTOR pathway. Am J Transl Res 11: 2042-2055, 2019.
67. Wei F, Jiang X, Gao HY and Gao SH: Liquiritin induces apoptosis and autophagy in cisplatin (DDP)-resistant gastric cancer cells *in vitro* and xenograft nude mice *in vivo*. Int J Oncol 51: 1383-1394, 2017.
68. Dikic I and Elazar Z: Mechanism and medical implications of mammalian autophagy. Nat Rev Mol Cell Biol 19: 349-364, 2018.
69. Masuda GO, Yashiro M, Kitayama K, Miki Y, Kasashima H, Kinoshita H, Morisaki T, Fukuoka T, Hasegawa T, Sakurai K, *et al*: Clinicopathological correlations of autophagy-related proteins LC3, beclin 1 and p62 in gastric cancer. Anticancer Res 36: 129-136, 2016.
70. Fan TJ, Han LH, Cong RS and Liang J: Caspase family proteases and apoptosis. Acta Biochim Biophys Sin (Shanghai) 37: 719-727, 2005.
71. Zhang Y, Yang X, Ge X and Zhang F: Puerarin attenuates neurological deficits via Bcl-2/Bax/cleaved caspase-3 and Sirt3/SOD2 apoptotic pathways in subarachnoid hemorrhage mice. Biomed Pharmacother 109: 726-733, 2019.
72. Choudhary GS, Al-Harbi S and Almasan A: Caspase-3 activation is a critical determinant of genotoxic stress-induced apoptosis. Methods Mol Biol 1219: 1-9, 2015.
73. Schroder K and Tschopp J: The inflammasomes. Cell 140: 821-832, 2010.
74. Zhang ZQ and Sun LL: Clinical significance of IL-1β and IL-18 in acute lung injury. Hainan Med J 28: 1954-1956, 2017 (In Chinese).
75. McVey MJ, Steinberg BE and Goldenberg NM: Inflammasome activation in acute lung injury. Am J Physiol Lung Cell Mol Physiol 320: L165-L178, 2021.
76. Karmakar M, Minns M, Greenberg EN, Diaz-Aponte J, Pestonjamasp K, Johnson JL, Rathkey JK, Abbott DW, Wang K, Shao F, *et al*: N-GSDMD trafficking to neutrophil organelles facilitates IL-1β release independently of plasma membrane pores and pyroptosis. Nat Commun 11: 2212, 2020.
77. Shi J, Gao W and Shao F: Pyroptosis: Gasdermin-mediated programmed necrotic cell death. Trends Biochem Sci 42: 245-254, 2017.
78. Liu Y, Zhou J, Luo Y, Li J, Shang L, Zhou F and Yang S: Honokiol alleviates LPS-induced acute lung injury by inhibiting NLRP3 inflammasome-mediated pyroptosis via Nrf2 activation in vitro and in vivo. Chin Med 16: 127, 2021.
79. D'Arcy MS: Cell death: A review of the major forms of apoptosis, necrosis and autophagy. Cell Biol Int 43: 582-592, 2019.
80. Tan S and Chen S: The mechanism and effect of autophagy, apoptosis, and pyroptosis on the progression of silicosis. Int J Mol Sci 22: 8110, 2021.
81. Ge Y, Xu X, Liang Q, Xu Y and Huang M: α-Mangostin suppresses NLRP3 inflammasome activation via promoting autophagy in LPS-stimulated murine macrophages and protects against CLP-induced sepsis in mice. Inflamm Res 68: 471-479, 2019.

82. Wong WT, Li LH, Rao YK, Yang SP, Cheng SM, Lin WY, Cheng CC, Chen A and Hua KF: Repositioning of the β-blocker carvedilol as a novel autophagy inducer that inhibits the NLRP3 inflammasome. Front Immunol 9: 1920, 2018.
83. Guo R, Wang H and Cui N: Autophagy regulation on pyroptosis: Mechanism and medical implication in sepsis. Mediators Inflamm 2021: 9925059, 2021.
84. Fernández A, Ordóñez R, Reiter RJ, González-Gallego J and Mauriz JL: Melatonin and endoplasmic reticulum stress: Relation to autophagy and apoptosis. J Pineal Res 59: 292-307, 2015.
85. Ma C, Zhang D, Ma Q, Liu Y and Yang Y: Arbutin inhibits inflammation and apoptosis by enhancing autophagy via SIRT1. Adv Clin Exp Med 30: 535-544, 2021.
86. Nakahira K, Cloonan SM, Mizumura K, Choi AMK and Ryter SW: Autophagy: A crucial moderator of redox balance, inflammation, and apoptosis in lung disease. Antioxid Redox Signal 20: 474-494, 2014.
87. Changle Z, Cuiling F, Feng F, Xiaoqin Y, Guishu W, Liangtian S and Jiakun Z: Baicalin inhibits inflammation of lipopolysaccharide-induced acute lung injury toll like receptor-4/myeloid differentiation primary response 88/nuclear factor-kappa B signaling pathway. J Tradit Chin Med 42: 200-212, 2022.
88. Liu Z, Wang P, Lu S, Guo R, Gao W, Tong H, Yin Y, Han X, Liu T, Chen X, *et al*: Liquiritin, a novel inhibitor of TRPV1 and TRPA1, protects against LPS-induced acute lung injury. Cell Calcium 88: 102198, 2020 (Epub ahead of print).